Bond Scission in a Perfect Polyethylene Chain and the Consequences for the Ultimate Strength

ARTICLE *in* MACROMOLECULES · NOVEMBER 2000

Impact Factor: 5.8 · DOI: 10.1021/ma000682a · Source: OAI

Bond Scission in a Perfect Polyethylene Chain and the Consequences for the Ultimate Strength

J. C. L. Hageman,*,† G. A. de Wijs,† R. A. de Groot,†,‡ and Robert J. Meier§

ESM, Research Institute of Materials, University of Nijmegen, Toernooiveld 1, 6525 ED Nijmegen, The Netherlands; Laboratory of Chemical Physics, Materials Science Center, Nijenborgh 4, 9747 AG Groningen, The Netherlands; and DSM Research, P.O. Box 18, 6160 MD Geleen, The Netherlands

Received April 19, 2000; Revised Manuscript Received September 7, 2000

ABSTRACT: We present ab initio calculations concerning the bond scission rate in a polyethylene chain. The energy barrier for scission is calculated both by using an effective potential scheme based on ab initio data and from the ab initio transition state itself. In the latter case the prefactor for scission is calculated. In both methods the relaxation of the polymer chain is taken into account, leading to a strong strain dependence of the energy barrier. The two schemes agree quantitatively. The barrier is reduced from 3.9 eV at zero strain to 1.7 eV at a strain of 5%. The calculated scission rate is used to estimate the strength of a polyethylene fiber consisting of perfectly aligned, independent chains in a constant strain rate experiment resulting in 18 GPa at a strain of 8%. This value of the ultimate strength is a factor 2 larger than found in experiments. This contrasts previously reported quantum chemical calculations, which reported values a factor 5−10 larger than the experimental values.

1. Introduction

The ultimate mechanical properties of high molecular weight ultraoriented polymer fibers are difficult to determine, as experimental samples suffer from defects that reduce the mechanical strength of the material, whereas theoretical calculations at an appropriate level of theory are almost absent. An overview of the ultimate properties of uniaxial polymer systems has been presented by Prevorsek.[1]

The ultimate modulus and tensile strength are properties of the ideal fiber consisting of perfectly aligned chains that span the whole fiber. In other words, they are the properties of the three-dimensional infinite crystal. Since the crystallographic unit cell for polyethylene (PE) is relatively small, one could have expected that a purely first-principles (ab initio) calculational approach at an appropriate level of theory would have been reported some time ago. This, however, is not the case. In fact, a few years ago results from a semiempirical quantum mechanical approach[2] were considered state-of-the-art.[3]

More recently, Hageman et al.[4] have reported the ultimate Young's modulus for orthorhombic PE based on a first-principles calculation. The calculation incorporated the full three-dimensional structure of the infinite polymer crystal. A modulus of 334 GPa was obtained for the experimental crystal structure at 4 K. The highest experimental value reported, 288 GPa measured at 77 K,[5] is lower than the calculated ultimate value. This is consistent, because the presence of defects in the real material and temperature effects will lower the modulus. Thus, a satisfactory theoretical upper limit has been obtained, and the difference between the ultimate value calculated and the highest experimental value reported is less than 15%.

Concerning the tensile strength, available quantum chemical[6−8] estimates (≈30−45% elongation at break and stress $\sigma \approx 34-66$ GPa) are far beyond what is observed experimentally. For ultrahigh molecular weight polyethylene fibers, i.e., ultradrawn material, values of 2−3% elongation at break and $\sigma \approx 7-8$ GPa[9−11] are measured. This discrepancy justifies other models of failure to be considered.

Apart from the useful early suggestions by Kausch and Becht,[12] Smith[13,14] has put forward an argument why the tensile strength at ambient temperature is much less than predicted on the basis of molecular calculations. The method employed by Smith to calculate the ultimate tensile strength is based on the thermodynamic stability range for different phases of the material (solid state, melt). It leads to an ultimate tensile strength close to 7.5 GPa at an elongation of 2.3%. In fact, the thermodynamic treatment presented by Smith suggests the onset of stress-induced melting to be responsible for failure. This result implies that the ultimately attainable tensile stress for the perfect polyethylene crystal is not really that much higher than the highest experimental values reported.

Alternatively, Crist et al.[15] have shown, for a model of coupled Morse oscillators, that the barrier for chain scission is reduced by relaxation of the nonbreaking bonds for the case of a constant strain. The reason this work, which could explain the discrepancy between theoretical and experimental ultimate strength, did not catch much attention is that it was generally assumed that fracture in polyethylene fibers occurred largely by chain slip and not by chain scission. In this paper we draw attention to this approach as this molecular level theory seems as irrefutable as Smith's macroscopic thermodynamic theory.

Another reason to look in more detail at the scission mechanism for fracture of a polyethylene fiber is the experimental result reported by Wang et al.[16] A significant number of radicals were detected under tensile load of polyethylene fibers, indicating bond scission to occur. This cannot be explained by a molecular process that contains solely chain slip, and hence the mechanism of chain scission should be considered.

† University of Nijmegen.
‡ Materials Science Center.
§ DSM Research.

10.1021/ma000682a CCC: $19.00
Published on Web 11/10/2000

Returning to the calculation of tensile strength, quantum mechanical calculations previously reported for polyethylene chains were either semiempirical in nature[8] or of the ab initio type.[6,7] In these calculations all CC bonds were kept identical upon straining the chains, and all CCC bond angles were also kept identical, implying that breaking of the chain was not observed explicitly. More in particular, the relaxation of the chain during the process of scission was not taken into account.

The recent first-principles molecular dynamical simulations of Saitta and Klein[17] focus on the influence of stress concentrations on fracture. They started with a simulation for a decane molecule (at finite temperature) and did allow for an inhomogeneous strain distribution during the scission process. They found a strain at failure of 18%. Although the inhomogeneous strain distribution allows for inclusion of the relaxation effect, the effect will be lower in decane than in polyethylene, since in decane only eight nonbreaking CC bonds can relax. The 18% strain at failure is, for that reason, not representative for polyethylene.

This work explicitly includes the relaxation of the chain as a whole and focuses on the bond scission as a function of the applied strain. The results of this single chain approach are used in a simple model for the ideal fiber—a fiber consisting of perfectly aligned chains that span the whole fiber—to estimate the ultimate strength. Interchain interactions are neglected. The calculated ultimate strength will be an upper bound for the strength of highly extended polyethylene fibers. This is an upper bound, since no weakening due to stress concentration effects is included, nor the effect of chain ends causing chain slip.

To describe the bond scission, the ideas of Crist et al.[15] are used to include the effect of the relaxation of the nonbreaking bonds. We extend their model in order to account for the full geometry of the polyethylene chain. This enables the use of ab initio calculations and results in a method that is appropriate for general linear polymers. More complicated polymers like polypropylene, nylon, or PBO could be treated in this framework as well as the weakening of a polyethylene chain due to side groups.

The physical quantity of interest is the rate of scission (ν) for bonds in the polyethylene chain. This is described by an Eyring rate equation:

$$\nu = \Omega e^{-\Delta E/k_B T} \tag{1}$$

where Ω is the prefactor depending on the entropy change, ΔE the energy barrier that is crossed, k_B the Boltzmann constant, and T the temperature.

We have calculated, by means of density functional theory (DFT), the energy barrier for bond scission in an ideal polyethylene chain as a function of the applied strain in two ways. First, we have used an effective potential based on ab initio calculations, which replaces the Morse potential in the model of Crist. Second, we have directly applied first-principles calculations in order to find the transition state at some particular strains. In one of these cases the prefactor Ω was also calculated. The barriers obtained by the two methods agree. Finally, the results on the barrier are used to estimate the time to break of an ideal fiber in a constant strain rate experiment.

2. Theory

The extension of the model of Crist is based on transition state theory. Before going into the details of the model, it is important to be convinced that a transition state exists, since this is the basic assumption in the extended model. For this, one has to realize that the initial state (i.e., the uniformly strained chain), which is a minimum of energy, is not the global minimum. This is easily demonstrated for a polymer chain with a fixed strain: To break a chain, one has to break one CC bond, which will cost about 4 eV (CC bond strength in ethane). After failure, all other bonds can relax so no elastic energy remains stored in these bonds. The energy of the broken chain will lie approximately 4 eV above the unstrained chain. In the case of the uniformly strained chain elastic energy will be stored in each bond. For a strain of 3% this is 20 meV per CC bond.[4] If the chain consists of 250 bonds, this is already larger than 4 eV; hence, for the infinite chain the broken chain is more favorable than a strained chain. From this reasoning it is clear that the uniformly strained, infinite chain is a local minimum on the energy surface and that the system can go to a lower minimum (the broken chain) by crossing a transition state, which is the saddle point on the energy surface between the two (local) minima.

The scission rate is the rate by which the chain crosses the transition state. Here it is assumed that the chain cannot recover from fracture. To calculate this rate, the physical properties at the two extrema of energy (the initial state and the transition state) have to be known. At these states there are no net forces; i.e., the energy gradients as a function of the atomic coordinates are zero. Since the chain ends are subjected to boundary conditions, a tension is allowed to exist in the chain. Like Crist et al.,[15] we treat two types of boundary conditions. First, a fixed external force is applied on the chain ends. Second, the chain is subjected to a fixed strain.

2.1. Fixed External Force. If a polymer chain is subjected to a fixed external force, work will be done by this force when the chain elongates while going to the transition state. To take this into account, the Gibbs free energy (G) should be used in the Eyring rate equation, which is written as

$$\nu = \frac{k_B T}{2\pi\hbar} e^{-\Delta G/k_B T} \tag{2}$$

where ΔG is the difference in the Gibbs free energy of the transition state and the initial state. For a rod under tension $G = A - fL$, where A is the Helmholtz free energy, f the external force, and L the length of the chain.

Statistical mechanics relates the Helmholtz free energy to the partition function $Z = e^{-A/k_B T}$. Near the initial state the partition function[18] can be written in the harmonic approximation as

$$Z^0 = \prod_{i=1}^{m} \frac{k_B T}{\hbar\omega_i^0} \tag{3}$$

where ω_i^0 are the vibrational eigenfrequencies corresponding with the m degrees of freedom. Here, the energy of the initial state is taken to be the zero of energy. The partition function can also be approximated

harmonically near the transition state, which has a potential energy ΔU with respect to the initial state. This approximation, with $\omega_i^{\ddagger}$ the vibrational frequencies at the transition state, is

$$Z^{\ddagger} = \mathrm{e}^{-\Delta U/k_\mathrm{B}T} \prod_{i=1}^{m-1} \frac{k_\mathrm{B}T}{\hbar\omega_i^{\ddagger}} \tag{4}$$

where the reaction coordinate is excluded from the product.

Writing the prefactor as

$$\Omega = \frac{1}{2\pi} \frac{\prod_{i=1}^{m-1} \frac{1}{\omega_i^{\ddagger}}}{\prod_{i=1}^{m} \frac{1}{\omega_i^{0}}} \tag{5}$$

the scission rate is given by

$$\nu = \Omega \mathrm{e}^{-(\Delta U - f\Delta L)/k_\mathrm{B}T} \tag{6}$$

Hence, to calculate the energy barrier

$$\Delta E = \Delta U - f\,\Delta L \tag{7}$$

one has to know the change in potential energy between the initial state and the transition state and the change in length at a fixed external force. The initial state is the uniformly strained chain whose tension balances this external force. Also, the tension at the transition in the chain state has to be equal to this external force. To calculate the prefactor, the vibrational spectra have to be calculated for both states.

From eq 7 it can be seen that the work done by the external force reduces the energy barrier. In the next part we demonstrate that for long polymer chains with constant length the same term appears, but then as a result of the relaxation of the nonbreaking bonds.

2.2. Fixed Length. For a polymer chain with fixed length, no work is done during the scission process, and eq 1 can be used to describe the scission rate. In this case ΔE is the potential energy difference between the initial state of the whole chain and the transition state of the whole chain.

To describe the chain, it is convenient to divide the N monomers into N_s segments with lengths L_i containing N_m monomers. The total length $L_\mathrm{tot} = \sum_i L_i$ is fixed. The assumption is made that the interaction between the segments can be described by the mutual response to changes in tension and lengths. This will be true if the segments are large enough.

The initial state is the uniformly strained chain. It is described by N_s equivalent segments. The length of each segment is L and the stress and energy are denoted by $\sigma(L)$ and $U(L)$, respectively. In Figure 1 this is drawn schematically. The total length of the initial state is $N_\mathrm{s}L$ and the total energy $N_\mathrm{s}U(L)$.

At the transition state there is one segment that contains the bond that will break, the breaking segment. All other segments respond to the changes in length and stress of this segment. They will be uniformly strained and all have a length L' and corresponding stress $\sigma(L')$ and energy $U(L')$, similar to the initial state (see Figure 1).

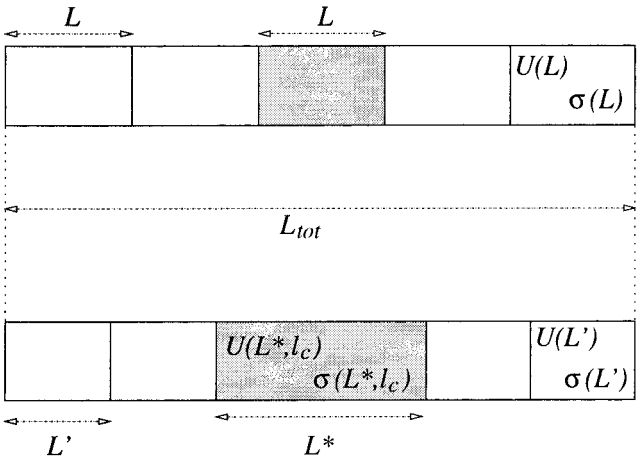

Figure 1. Schematic representation of the uniformly strained chain and the transition state in the case of a fixed total length L_tot. The chain is divided in five segments. The upper part of the figure represents the uniformly strained chain where all segments have the same length L. The lower part represents the transition state, where the breaking segment (gray rectangle) has length L^*. The other segments have to shrink to L' in order to ensure a constant total length of the chain. The energies and stresses of the segments are also shown. The parameter l_c is defined in the text and in Figure 4a, where it is equal to l_const for zero $\mathbf{F}_\mathrm{const}$.

The breaking segment is special and should be treated separately. In this segment one bond will be much longer than the other bonds. The length of the projection of this bond on the chain axis is denoted by l_c. The length of the segment is L^*. It is assumed that the parameters l_c and L^*—together with the condition that there are no net forces in the chain—are sufficient to characterize this segment.[19] The stress and energy are written as $\sigma(L^*,l_\mathrm{c})$ and $U(L^*,l_\mathrm{c})$, respectively. The total length of the chain at the transition state is $L^* + (N_\mathrm{s} - 1)L'$ and the total energy $U(L^*,l_\mathrm{c}) + (N_\mathrm{s} - 1)U(L')$.

Defining $\Delta L = L^* - L$, which is the difference between the length of the breaking segment at the transition state and at the initial state, the relation between L' and L is given by

$$L' = L - \frac{\Delta L}{N_\mathrm{s} - 1} \tag{8}$$

The energy barrier, which is the energy difference between the transition state and the initial state, then is

$$\begin{aligned} \Delta E &= U(L^*,l_\mathrm{c}) + (N_\mathrm{s} - 1)U(L') - N_\mathrm{s}U(L) \\ &= U(L+\Delta L,l_\mathrm{c}) - U(L) + \\ &\qquad (N_\mathrm{s} - 1)\left[U\left(L - \frac{\Delta L}{N_\mathrm{s} - 1}\right) - U(L)\right] \end{aligned} \tag{9}$$

For large N_s this is

$$\Delta E = U(L+\Delta L,l_\mathrm{c}) - U(L) - \Delta L \frac{\mathrm{d}U(L)}{\mathrm{d}L} \tag{10}$$

Using $\Delta U = U(L+\Delta L,l_\mathrm{c}) - U(L)$ and the fact that the derivative of the energy to the length is the tension f:

$$\Delta E = \Delta U - f\,\Delta L \tag{11}$$

This is exactly the same expression as in the case of a constant external force, but now derived from a relax-

ation mechanism. The prefactor is described by eq 5 for constant strain as well as for constant force, since it depends only on the ratio of the partition functions of the transition state and initial state.

It is important to realize that the energy difference ΔU of eq 7 is the same as that of eq 11 for large N_s, although they are defined differently. In eq 11, it is the energy difference between the transition state and the initial state of the breaking segment. In eq 7, it is the energy difference of the chain between the transition state and the initial state. However, in this case the nonbreaking segments will not change, because they are subjected to the same force at the transition state and initial state. Hence, the change is located in one segment, and the energy difference of the chain is equal to the energy difference of the breaking segment. A similar reasoning holds for the change of length. Also, it should be realized that for the infinite chain the change in tension is negligible.

2.3. Implementation of the Theory. In the previous part, a general formalism was obtained to derive the scission rate. Irrespective of the boundary conditions on an infinite chain, the scission rate can be calculated from the potential energy, the length, and the vibrational spectrum of the breaking segment at the transition state and at the initial state. The transition state and the initial state are defined by the requirement that they share the predefined tension.

Three strategies are distinguished in the implementation of the theory:

1. *The model of Crist* is retrieved by assuming that the energy of a uniformly strained segment is the same as the energy of a segment containing one elongated bond, that is $U(L) = U(L,l_c)$. The energy is given by the Morse potential $V_M(L)$, which is a reasonable approximation. Since there is no difference in behavior of a segment and a bond, they cannot be separated. For this reason L can be considered to be the length of a bond in the chain direction. Then, the barrier is

$$\Delta E = V_M(L+\Delta L) - V_M(L) - \Delta L \left.\frac{dV_M}{dL'}\right|_{L'=L+\Delta L} \quad (12)$$

where ΔL is defined by the condition that

$$\left.\frac{dV_M}{dL'}\right|_{L'=L+\Delta L} = \left.\frac{dV_M}{dL'}\right|_{L'=L} \quad (13)$$

2. *The effective potential scheme.* The model of Crist can be improved by replacing the Morse potential by a more specific potential $V_{eff}(L)$. This potential describes the energy of a bond in the polyethylene chain and can be calculated using fits to ab initio data. A further improvement is to assume that the potential of the breaking bond depends on the strain of the other bonds $[V_{eff}(L,\epsilon)]$ and to recalculate the barrier for different strains. In this way, the next-nearest-neighbor interaction can be incorporated in a mean field approach.

3. *The ab initio transition state.* It is not necessary to introduce an effective potential, however. The theory can be applied directly to ab initio calculations. The transition state has to be found by geometry optimizations under the constraint of having one breaking bond. The energy $U(L^*,l_c)$ is associated with the energy of this transition state. $U(L)$ is the energy of a uniformly strained chain with the same stress as the transition state. Since we are using density functional theory to evaluate the energies and forces, this barrier is a truly first-principles barrier. Although this scheme is more accurate than the effective potential method, it is less straightforward to control the strain for which the barrier is calculated.

3. The Energy Barrier

Two of the schemes described above are used to calculate the energy barrier: the effective potential scheme (2) and the method of finding the ab initio transition state (3). For both schemes ab initio calculations are performed.

3.1. Computational Details. All the calculations presented in this work have been performed using the ab initio total energy and molecular dynamics program VASP[20−22] (Vienna Ab initio Simulation Program) developed at the Institut für Theoretische Physik of the Technische Universität Wien. To describe the behavior of the electrons, density functional theory (DFT) is used in the generalized gradient approximation (GGA) of Perdew and Wang.[23] Spin polarization was applied (when necessary) since radicals are formed during scission. The atomic cores are described with ultrasoft Vanderbilt pseudopotentials,[24] and a plane wave basis set including waves with a kinetic energy up to 26 Ry is sufficient for the wave functions.

To check whether DFT-GGA describes the strength of a CC bond sufficiently accurate, the energy difference between C_2H_6 and $2 \times CH_3$ is calculated, resulting in 4.24 eV. The experimental value of this energy difference can be obtained from the well-known bond dissociation enthalpy for ethane[25] (3.81 eV) and correcting this for the zero point motion of the atoms. Using the vibrational frequencies for ethane[26] and the CH_3 radical,[27] this leads to an "experimental" bond strength of 4.20 eV. The calculated strength is in good agreement with this value.

The polyethylene chain is described by a unit cell with periodic boundary conditions containing a $C_{10}H_{20}$ segment. The unit cell has a size of 9 Å × 9 Å × L_u, where L_u is the appropriate length for the chain. One **k**-point, $(0,0,^1/_4)$, is sufficient to represent the Brillouin zone integral since the unit cell is long and the interchain interaction can be neglected due to the large area. For the uniformly strained chain we have fitted the Murnaghan equation of state[28] to the energy as a function of the length L_u like in previous work:[4]

$$E(L_u) = \frac{AY_0L_u}{Y_1(Y_1-1)}\left[Y_1\left(1-\frac{L_0}{L_u}\right) + \left(\frac{L_0}{L_u}\right)^{Y_1} - 1\right] \quad (14)$$

and found the coefficients

$$L_0 = 12.79 \text{ Å}, \quad AY_0 = 34.60 \text{ eV Å}^{-1}, \quad Y_1 = 5.65 \quad (15)$$

Using the room-temperature area per chain of $A = 18.24$ Å^2 results in a Young modulus of 300 GPa. This result is smaller than our previous result of 320 GPa.[4,29] This effect is expected since the generalized gradient approximation is used here instead of the local density approximation. We have found a similar effect for the rigid-rod polymer PIPD.[30] The length of the primitive cell at equilibrium ($L_0/5$) is found to be 2.56 Å, somewhat larger than the experimental value (2.53 Å) and our previous result (2.51 Å). Again, this is in agreement with expectations for GGA.

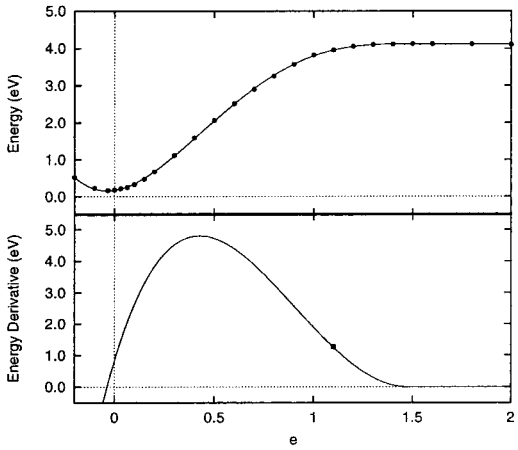

Figure 2. Effective potential (eq 16) and its derivative are depicted in the top and bottom figure, respectively. The top figure shows the ab initio energy as full circles and the least-squares fit of V_{eff} to these data as solid line, both as a function of the strain e of the breaking bond (as defined in the text). In the bottom figure the derivative of V_{eff} with respect to the length of the breaking bond is shown as a solid line. The full square is the point where the derivative becomes (again) equal to the force in the uniformly strained chain. The corresponding strain is applied to the breaking bond at the transition state.

The combination of a good "potential depth" and a correct elastic modulus makes the DFT-GGA suitable to calculate the energy barrier.

3.2. The Effective Potential Scheme. In section 2.3 one bond plays the role of parameter in the effective potential. More precisely, the length of the projection of this bond on the chain direction, i.e., the strain in this bond, can be used as the parameter L in $V_{\text{eff}}(L,\epsilon)$. The unit cell as described above, containing 10 CC bonds, is used, and the effective potential is identified with the energy of this unit cell as a function of L. The strain of the other nine bonds is kept fixed at $\epsilon = 0.032$. Hence, the length of the unit cell is $L_u = L + (9/10)(1 + \epsilon)L_0$. The CC bonds are allowed to relax perpendicular to the chain, and also the CH bonds are allowed to relax. The effective potential created in this way is $V_{\text{eff}}(L,\epsilon{=}0.032)$.

The energy of the unit cell is calculated for different L; the data are shown in Figure 2. The zero of energy is taken to be the unstrained chain. The data are used to make a linear least-squares fit of the effective potential described by

$$V_{\text{eff}}(L) = \sum_{m=0}^{5} V_m e^m \qquad \text{for } e \le q \qquad (16)$$

$$= V_b \qquad \text{for } e \ge q$$

where V_m, V_b, and q are the fitting parameters and the strain in the breaking bond $e = (L - l_0)/l_0$ with $l_0 = 1.279$ Å. V_{eff} has to be continuous in e at q, as well as its first and second derivative. Thus, not all parameters are free. All are given in Table 1. The fact that the curve does not have its minimum at $L = l_0$ is an indication that the strain in the other bonds is important. For this reason it is better to describe the tension f at the initial state with the derivative of eq 14 and not with the derivative $V'_{\text{eff}}(L = (1 + \epsilon)L_0)$.

Since the effective potential describing the breaking bond is now determined, the model can be used to calculate the energy barrier for $\epsilon = 0.032$: The length of the initial state is $L = (1 + \epsilon)l_0$. Its energy is $U(L) = V_{\text{eff}}([1 + \epsilon]l_0)$, and its tension is f (determined from eq 14). The transition state has to have the same tension f. The point where the derivative of the effective potential becomes equal to this tension is presented by the full square in Figure 2. The corresponding length is L^*, and the energy is given by $U(L^*) = V_{\text{eff}}(L^*)$. Using eq 11, this results in an energy barrier of 2.377 eV.

Table 1. Parameters V_m (in eV) and q (Dimensionless) Describing the Effective Potential $V_{\text{eff}}(L)$ for a Strain of 0.032[a]

V_0	0.172	V_1	0.837
V_2	10.685	V_3	−11.748
V_4	4.319	V_5	−0.470
q	1.475	V_b	4.117

[a] The parameters are obtained from a least-squares fit to the energy as a function of the length L of the breaking bond. The energies are obtained with ab initio calculations. The zero of energy is taken to be the unstrained chain.

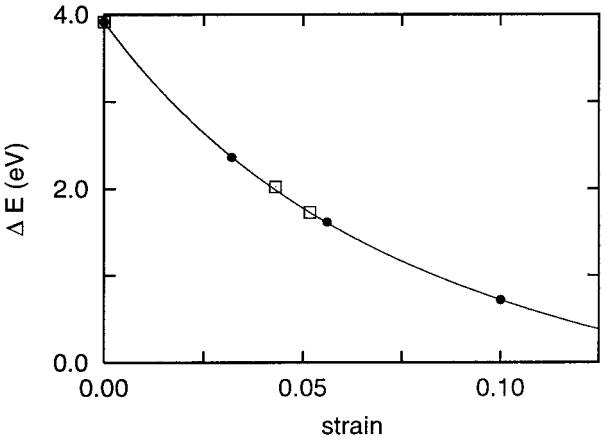

Figure 3. Energy barrier is plotted as a function of the applied strain. The full circles are the data resulting from the effective potential scheme. The solid line is the least-squares fit of eq 17 to these data. The open squares are the results from the ab initio search for the transition state, as discussed in section 3.3.

The effective potential depends on the strain ϵ and is calculated for $\epsilon = 0.032$. It will only be valid in the neighborhood of $\epsilon = 0.032$. For this reason, we have repeated the ab initio calculations for the uniform strains of 0.000, 0.056, and 0.100. In these cases, only seven well-chosen points are used, and m was taken to be up to 4, which gives accurate enough results. (For a strain of 0.032 this gives $\Delta E = 2.372$ eV.) The resulting barriers are shown in Figure 3 as full circles. The dependency can be described with a quadratic function in the stress $\sigma = f/A$, which is

$$\sigma = \frac{Y_0}{Y_1}\left[1 - \left(\frac{1}{1+\epsilon}\right)^{Y_1}\right]$$

from eq 14, namely

$$\Delta E = \Delta E_0 - \gamma_1\sigma + \gamma_2\sigma^2 \qquad (17)$$

with $\Delta E_0 = 3.91$ eV, $\gamma_1 = 0.197$ eV/GPa, and $\gamma_2 = 2.42 \times 10^{-3}$ eV/GPa^2. This is shown in Figure 3 as the solid line. The term ΔE_0 can be interpreted as the strength of a CC bond in polyethylene, which is a reasonable value compared to the bond strength in ethane (4.20 eV). The dependence of the barrier on the

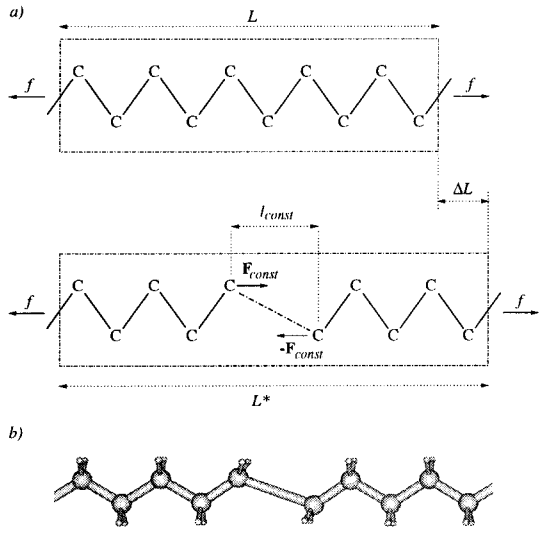

Figure 4. (a) Schematic representation of the procedure to find the transition state and the initial state. The hydrogen atoms are left out of the scheme for clarity. The top of the figure represents the initial state. In the lower part of (a) the search for the transition state is depicted. The symbols are explained in the text. (b) The transition state for $L^* = 14.57$ Å is shown. The axis of the chain is rotated over a small angle out of the page in order to show all hydrogen atoms. The elongated, breaking bond is clearly visible. Notice that the hydrogen bonds near the breaking bond are rotated toward the breaking bond and that the bonds next to the breaking bonds are shorter than the others.

strain is strong; at a strain of 0.032 the barrier has dropped as much as 40%.

3.3. The ab Initio Transition State. In the previous part we fixed the strain in the nonbreaking bonds. This implies the presence of constraining forces. Consequently, only an approximation to the transition state was found. Although this might be a good approximation, this is not proven yet. Moreover, it prevents us from calculating the proper frequencies for the transition state. Finally, there is no fundamental reason to use the intermediate of an effective potential.

In this part ab initio calculations are used to find the transition state of the breaking segment. That is the state of the unit cell containing the $C_{10}H_{20}$ group for which all atoms are in equilibrium positions (no constraining forces) and one bond is much elongated. The only constraint is the length of the unit cell. This unit cell plays the role of the segment described in the theory of section 2. We apply periodic boundary conditions to this segment and check whether this is allowed afterward. When the energy, length, and tension at the transition state and at the initial state are known, the energy barrier can be calculated using eq 11.

In the search for the transition state we have fixed the length of the unit cell. A good estimate for an appropriate length can be obtained from the effective potential scheme. In that case, the length of the projection on the chain direction of the breaking bond was 2.69 Å at the transition state for a strain of 0.032. For the other bonds this length was 1.32 Å. Hence, in a unit cell of $L_u = 14.57$ Å a transition state is expected with a reasonable tension. This length corresponds with L^* from section 2.2.

The procedure to find the transition state in this unit cell was the following (see also Figure 4): the breaking bond was elongated much, and the length of its projection on the chain direction was kept fixed at l_{const}. All other atomic coordinates were optimized until the corresponding net forces had vanished. Only the constraining forces $\mathbf{F}_{const}$ resulted. Then the constraining length l_{const} was changed, while reoptimizing the other coordinates, until also the constraining forces $\mathbf{F}_{const}$ vanished, leading to the transition state. At the transition state the unit cell had an energy $U = 3.93$ eV and a tension $f = 2.43$ nN for a length $L^* = 14.57$ Å.

Table 2. Bond Lengths (in Å) and Bond Angles (in deg) around the Breaking Bond at the Transition State (TS) and the Initial State (IS)[a]

	TS 5.2%	IS 5.2%	TS 4.3%	IS 4.3%
C···C	2.76	1.58	2.82	1.57
C−C(···)	1.53	1.58	1.52	1.57
C···C−C	126	117	125	117
H−C−H	114	106	115	106
H−C−C	117	108	118	108

[a] The data are shown for both calculations, corresponding to initial strains of 5.2% and 4.3%. The dots indicate the breaking bond.

To calculate the barrier, the length and energy of the initial state, i.e., the appropriate uniformly strained segment, have to be known. This unit has to have the same tension as the unit corresponding to the transition state ($f = 2.43$ nN). The derivative of eq 14 is used to find the length of the uniformly strained segment, $L = 13.46$ Å. The energy for this length is calculated to be $U = 0.51$ eV. The actual stress is 2.35 nN, which is close to 2.43 nN.

These data for the transition state and the initial state result in the energy difference $\Delta U = 3.42$ eV, the term $f\Delta L = 1.69$ eV, and the barrier $\Delta E = 1.73$ eV. The applied strain to which this barrier belongs is the same as the initial strain (5.2%).

A measure of the validity of the application of periodic boundary conditions is the difference between the length of the projection of the bonds in the uniformly strained case and this length of the bond farthest apart from the breaking bond in the case of the transition state. This difference is smaller than 0.001 Å.

For a slightly smaller unit cell ($L_u = 14.50$ Å) the procedure was repeated. This resulted in $\Delta U = 3.49$ eV, $\Delta L = 1.16$ Å, and $\Delta E = 2.02$ eV at an initial strain of 4.3%. Both barriers are depicted as open squares in Figure 3. These results clearly agree with the effective potential scheme for the size of the barrier.

In Figure 3 a third open square is shown at zero strain. This barrier is the energy of the broken segment. It is calculated by using a large unit cell ($L = 16.8$ Å) and one bond broken. Relaxation of all other bonds gives an energy difference of 3.91 eV, which is the barrier for scission without any strain. This is exactly the same result as for the effective potential method.

Some interesting details of the atomic configuration at the transition state should be mentioned. In Table 2 some important bond lengths and angles are given. The configuration is visualized in Figure 4 for the 14.57 Å cell. The bonds and bond angles in the initial states are very similar. This is expected since their strains differ less than 1%. It is noteworthy that the length of the breaking bond at the transition state in the 14.50 Å cell is larger than the one in the 14.57 Å cell. We can understand this in the following way: the breaking bond is elongated so much that the stress in the bond will decrease upon further elongation. The stress in the 14.57 Å cell is the larger one, and hence the breaking bond is shorter than in the 14.50 Å cell.[31]

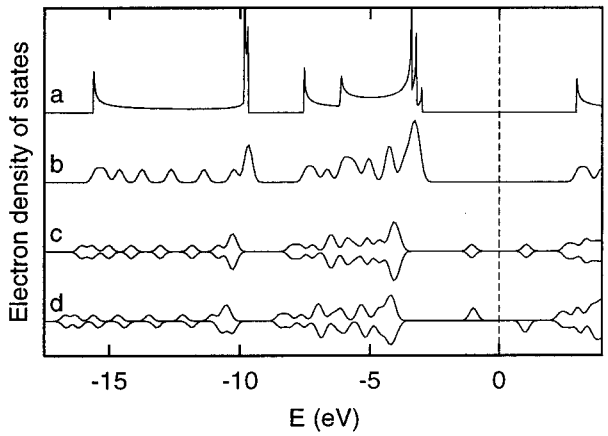

Figure 5. Electron density of states (EDOS). All electron states below zero are occupied; above zero they are unoccupied. Line a is the accurate EDOS for the uniformly strained chain. Lines b−d are the EDOS at the **k**-point $(0,0,^1/_4)$ used for the geometry optimizations. Line b shows the EDOS in the case of the uniformly strained chain. The EDOS of the transition state (line c) is divided into two spin channels. One is plotted with positive intensity and the other with negative intensity. The EDOS of the broken chain is line d.

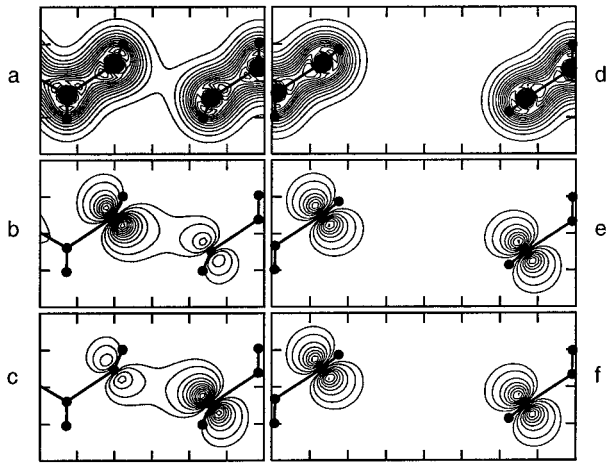

Figure 6. Electronic densities around the breaking bond. Figures a and d display the total electron density for the transition state and the broken chain, respectively. The plotted contours shown are $n \times 0.143$ el/Å^3 with $n = 0, 1, ..., 12$. The two highest occupied molecular orbitals of the transition state are shown in parts b and c. Those of the broken chain in parts e and f. The contours plotted in parts b, c, e, and f are 0.03575 el/Å^3 and $n \times 0.0715$ el/Å^3 with $n = 1, 2, ..., 10$. The distance between tics is 1 Å.

The electronic structure gives more insight into the mechanism of scission. In Figure 5 electron densities of states (EDOS) are plotted for the initial state at $L =$ 13.46 Å, the transition state at $L = 14.57$ Å, and the broken chain at $L = 16.8$ Å.

Figure 5a visualizes the accurate EDOS for the uniformly strained chain and is shown for reference. It is calculated in the primitive unit cell with 61 **k**-points using linear interpolation for the energy bands. Figure 5b is also the EDOS for the uniformly strained chain in the large unit cell, but only at the **k**-point used for the geometry optimization. The energy levels are smeared by a Gaussian of 0.2 eV width. Both densities of states show basically the same features at the same energies, and since the physical quantities in this paper depend on integrals over all occupied states, one **k**-point is sufficient.

Figure 5c displays the EDOS for the transition state, where spin polarization is applied. The two spin directions give degenerate energy levels. Four states lie in the energy gap. Two states (of opposite spin) are occupied and are shown in Figure 6b,c. They have clearly a large p character and are localized on the carbon atoms forming the breaking bond. The orbital shown in Figure 6b is of the bonding type, since there is a significant amount of charge between the carbon atoms. This is expected as the breaking bond has to support the stress in the chain. The two unoccupied states in the gap are the antibonding counterparts of the occupied states.

Also, the process of radical formation can be seen in Figure 6b,c: one spin is more localized on the left carbon atom than on the right. Upon increasing the distance, it will become even more localized on the left carbon atom. The orbital of Figure 6c will form the radical on the right carbon atom.

In the case of the broken chain (Figures 5d and 6d−f), the highest occupied molecular orbitals have the same spin in accordance with Hund's rule. They are again localized on the carbon atoms "forming" the broken bond and are mainly of p character. The orientation is almost perpendicular to the plane of the carbon atom and the hydrogen atoms attached. The two orbitals are nearly degenerate but have a splitting of 0.08 eV. This is caused by a small interaction due to the finite size of the unit cell, resulting in a small bonding−antibonding splitting. In the case of the infinite chain the two orbitals would be degenerate, and they may be mixed in such a way that one orbital describes a radical on the left carbon atom and the other on the right carbon atom.

4. The Prefactor

In this part the vibrational spectra are calculated and used for the determination of the prefactor. This is performed in the case of the tension of 2.43 nN as used in the previous section. Since there are no residual forces, a force constant approach[32] can be applied.

4.1. Computational Details. The phonon frequencies are calculated in the harmonic approach by constructing the dynamical matrix in the form

$$D_{ij}^{rs}(k) = K_{ij}^{rs} e^{iknL_u}/\sqrt{M_i M_j} \tag{18}$$

where K_{ij} is the harmonic force constant between the atoms i and j; r and s give the directions of the corresponding displacements. M_i is the mass of atom i, L_u is the length of the unit cell, k is the wave vector, and n labels whether atom j is in the same supercell ($n = 0$) as i, in the next unit cell ($n = 1$), or in the preceding unit cell ($n = -1$).

To calculate the harmonic force constants, the atom i is displaced over $d_i^s = 0.02$ Å in the direction $s = x, y,$ or z, and the resulting forces $\mathbf{F}_j$ are calculated from first principles. The force constants $K_{ij}^{rs} = F_j^r/d_i^s$ are averaged over positive and negative displacements, giving harmonic force constants. All the available symmetry of the polyethylene chain is used in order to reduce the number of displacements necessary to construct the dynamical matrix. The symmetry properties of the dynamical matrix are used to remove the effects of overdetermination.

Diagonalization of the dynamical matrix results in the eigenfrequencies as a function of k.[33] Integrating over

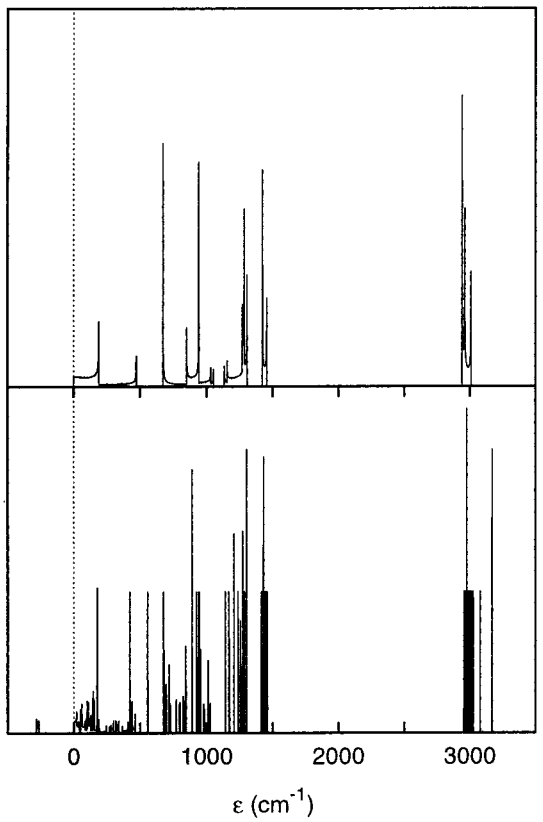

Figure 7. Phonon density of states for the uniformly strained chain (upper panel) and the transition state (lower panel) as a function of the vibrational energy. Both densities of states are in the same arbitrary units. Imaginary frequencies are displayed as negative values.

the Brillouin zone results in a phonon density of states $G(\epsilon)$ with the vibrational energy $\epsilon = \hbar\omega$. The Brillouin zone integrals are calculated as summations over histograms of the spectrum at 4096 k-points with an energy resolution of 1 cm^{-1}.

4.2. Results. The procedure to calculate phonon frequencies as described above is validated by checking the CC stretching modes for the unstrained chain. For the asymmetric stretch a frequency of 1052 cm^{-1} is found, for the symmetric stretch a frequency of 1115 cm^{-1}. This is in close agreement with the experimental values from Raman spectroscopy, which are 1061 and 1128 cm^{-1}, respectively.[34]

We have calculated the spectra for the transition state in the supercell with $L = 14.57$ Å and the corresponding uniformly strained chain. Both are shown in Figure 7. The spectrum of the uniformly strained chain is similar to the spectrum of the unstrained chain. The asymmetric CC stretch is shifted 110 cm^{-1} downward and the symmetric stretch, 64 cm^{-1}. If we divide the shift for the symmetric mode by the stress, we obtain the shift per unit stress of 4.18 cm^{-1} GPa, which is in excellent agreement with the experiments of Prasad and Grubb[35] (4 cm^{-1} GPa). The shift per unit strain for the symmetric mode is 12.5 cm^{-1}/%. This is higher than the value of Moonen et al.[36] (8.7 cm^{-1}/%), which is corrected for the discrepancy between the macroscopic and microscopic strains, and the calculated value of Meier et al.[37] (8.0 cm^{-1}/%).

The spectrum of the transition state is very spiky. There is one imaginary frequency band (≈275 cm^{-1}), the soft mode. Its dispersion is small (17 cm^{-1}), illustrating that the unit cell has been chosen large enough.

The prefactor is calculated from the above spectra in two ways. First, only the data at $k = 0$ (Γ) are used in eq 5, which results in a prefactor of $\Omega = 1.4 \times 10^{15}$ s^{-1}. Second, the density of states is used, which is the same as integrating over the Brillouin zone. To do this, the logarithm of the prefactor is rewritten as

$$\ln(\Omega) = -\ln(h/k_B T) + \int_0^\infty [G^\ddagger(\epsilon) - G(\epsilon)] \ln[z(\epsilon)]\, d\epsilon \tag{19}$$

where G and $G^\ddagger$ are the phonon density of states for the uniformly strained chain and the transition state, respectively, and $z(\hbar\omega) = k_B T/\hbar\omega$ the classical partition function for a single oscillator. This results in a prefactor $\Omega = 2.1 \times 10^{15}$ s^{-1}, which is in good agreement with the value for Γ. Because of dispersion, the partition function for the uniformly strained chain approximated by the summation at Γ is not the same as the integral over the Brillouin zone.

These values can be compared with a common estimate assuming that the only change in the spectrum is the change of a mode into the soft mode. Then, all other frequencies in eq 5 cancel and the prefactor can be written as $\Omega = \omega/2\pi$. Since the soft mode will correspond with a separation of two CC atoms, it is reasonable to take a CC stretch mode, i.e., $\omega \approx 1100$ cm^{-1}. This results in a prefactor $\Omega = 3.2 \times 10^{13}$ s^{-1}, almost 2 orders of magnitude lower than the prefactors above. This discrepancy can be understood from the vibrational spectrum. The change in the spectrum is not only a CC stretch mode that becomes the soft mode. In addition, there are two modes, which involve the rotation around the axis of the breaking bond, that lower in energy. This leads to an enhancement of the breaking rate.

Since the phonon spectra are available now, the energy of the zero point motion of the atoms can be calculated. The energy of the initial state is shifted $\sum_{i=1}^{m} {}^1/_2\hbar\omega_i^0$ upward. The energy of the transition state is shifted by $\sum_{i=1}^{m-1} {}^1/_2\hbar\omega_i^\ddagger$. This would lead to a change in energy difference of −0.17 eV. This is less than the energy difference between the zero point motions in the case of ethane and two CH_3 radicals, which is −0.39 eV, but still significant.

It seems straightforward to add the change in energy difference to the initial barrier and take this as a quantum mechanical correction. However, actually the influence of quantum effects should be estimated by calculating the prefactor with the quantum mechanical partition function, which is

$$z(\hbar\omega) = \frac{\exp[-{}^1/_2\hbar\omega/k_B T]}{1 - \exp[-\hbar\omega/k_B T]} \tag{20}$$

The numerator in this equation accounts for the zero point motion.

Using this expression for the partition function in eq 19, the prefactor turns out to be no longer temperature independent. For $T = 300$ K it is 2.4×10^{16} s^{-1}, an order of magnitude larger than the prefactor using the classical partition function. For the temperature range of 250−350 K the prefactor can be described as $\Omega = \tilde{\Omega} \exp[-\Delta E^{QM}/k_B T]$, with $\tilde{\Omega} = 2.0 \times 10^{14}$ s^{-1} and $\Delta E^{QM} = -0.124$ eV. The use of this prefactor $\tilde{\Omega}$ and correcting the initial barrier with the energy ΔE^{QM}, leading to $\Delta E_0 = 3.79$ eV, can be seen as a quantum mechanical correction to the scission rate. Note that this energy

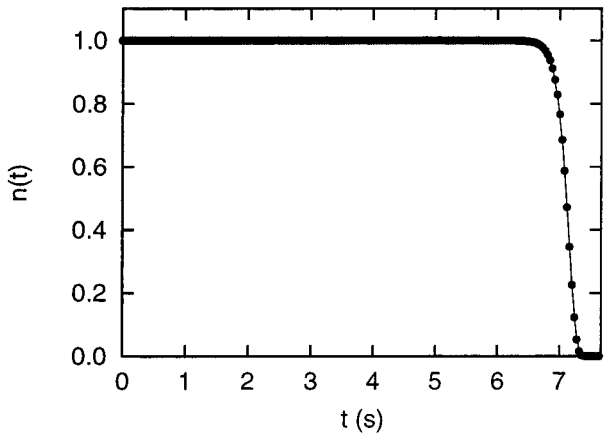

Figure 8. Fraction of nonbroken chains in a constant strain rate experiment for the independent chain model. The chains contain 10 000 CC bonds and are subjected to a strain rate of 0.011 s^{-1} at a temperature of 300 K. The full circles are the results of the numerical integration of eq 21. The solid line is the function of eq 22, showing excellent agreement.

correction is smaller than the change due to the zero point motion.

5. The Ultimate Strength

In the previous part the barrier was calculated as a function of the strain (eq 17). Together with the prefactor $\Omega = 2.1 \times 10^{15}$ s^{-1} this gives the scission rate. Although this is an important result, it does not give the ultimate strength directly.

To get a good impression of the effect of the strong strain dependence of the barrier on the ultimate strength, a simple model for the fiber is used to estimate the strain at failure in a constant strain rate experiment. This results in a prediction of the ultimate strength based on chain scission. In the model interchain interactions are neglected, and this will lead to an upper bound for the strength of real fibers, since no stress concentrations are considered. The upper bound will be relevant for highly extended chain fibers consisting of very long molecular chains.

The model of the ideal fiber used is a collection of N_k perfectly aligned, independent chains, each consisting of N_b bonds. The scission rate $\nu(\epsilon)$ is the rate by which a chain will cross a specific transition state. A chain that has N_b bonds has N_b of such transition states. Hence, the rate for a chain to cross any transition state is $\tilde{\nu}(\epsilon) = N_b\nu(\epsilon)$. If a chain has crossed a transition state, it is considered to be broken.

The applied strain is time-dependent: $\epsilon = \dot{\epsilon}t$, where $\dot{\epsilon}$ is the constant strain rate and t the time. Hence, the rate of scission will be time dependent, too. $N_k(t)\,\tilde{\nu}(\dot{\epsilon}t)\,dt$ chains will break between time t and $t + dt$. Hence, the fraction of nonbroken chains ($n(t) = N_k(t)/N_k(0)$) at time t is

$$n(t) = 1 - \int_0^t n(t')\,\tilde{\nu}(\dot{\epsilon}t')\,dt' \qquad (21)$$

This equation can be integrated numerically. The result is shown in Figure 8 for a strain rate of $\dot{\epsilon} = 0.011$ s^{-1}, $T = 300$ K, and $N_b = 10\,000$. Between 0 and 6 s nothing happens, and suddenly all chains break within 1 s. Equation 21 suggests a function like

$$n(t) = e^{-e^{\tilde{\nu}(\dot{\epsilon}\tau)(t-\tau)}} \qquad (22)$$

This is also shown in Figure 8. If the time τ is taken to be the time for which $n(\tau) = 1/e$, it turns out to be an excellent description of the process, and we take τ to be the time of fracture for the fiber consisting of independent chains. The strain at fracture $\epsilon = \dot{\epsilon}\tau$ is 0.078, and the stress σ is 18.6 GPa. If the quantum mechanical corrections to the prefactor and the energy are applied ($\Omega = \tilde{\Omega} = 2.0 \times 10^{14}$ s^{-1} and $\Delta E_0 = 3.79$ eV), then the strain at failure is 0.075 and the stress 18.0 GPa. For both this is a reduction of approximately 3%.

Strain rate, temperature, and number of bonds all influence the strain at failure, since the chain scission rate $\tilde{\nu}$ depends on them. However, for strain rates from 0.001 to 0.011 s^{-1} the strain at fracture only changes from 0.076 to 0.078 and can be considered constant. The influence of temperature is somewhat larger; the strain at fracture changes from 0.099 to 0.062 when temperature changes from 200 to 400 K. Changing the number of bonds from 10 to 10^9 results in strains from 0.088 to 0.065.

It is remarkable that the strain at failure—and hence the time of fracture—are in reasonable agreement with the experiment of Smith and Lemstra[38] for fibers with moduli between 17 and 90 GPa. In their constant strain rate experiment they find strains at break between 0.090 and 0.059. Recently, Wang et al.[11] have performed a similar experiment at a strain rate of 0.00667 s^{-1} for fibers with moduli between 13 and 246 GPa, resulting in strains between 0.097 and 0.034. It should be noted that these strains are macroscopic strains of the fibers and not microscopic strains on the chains, which are different for imperfect fibers. The lower strains at failure are found in the higher modulus fibers. Hence, the ideal fiber, with the highest possible modulus, is expected to fail at a strain lower than 0.034. This is approximately a factor of 2 lower than the strain calculated. Also, there is a difference between the measured stresses at fracture, 0.73−3.04 GPa[38] and 0.97−7.15 GPa[11] in the two experiments, and the stresses found in the chains in our fiber, which are of the order of 18 GPa.

Despite its simplicity, this model gives us some important results: if we write the time to break as a Zhurkov[39] equation

$$\tau = \tau_0 e^{\Delta U/k_B T} \qquad (23)$$

and we take $\tau_0 = 10^{-13}$ s, we find for the above example an activation energy $\Delta U = 0.82$ eV. First, we note that this barrier is 5 times smaller than the energy of a CC bond. *Usually, small values of the activation energy in experiments are interpreted to be an argument against the mechanism of chain scission.*[14,38] *Since the latter is the only mechanism involved in failure of our fiber and we find such a low activation energy, this interpretation should be abandoned.* Second, the barrier for scission at the time of fracture is $\Delta E = 1.09$ eV (eq 17), which is clearly not the same as ΔU. This means that the activation energy and the barrier for scission are not equivalent, although scission is the mechanism involved.

If the model is changed slightly it can be used to describe a constant strain experiment. The chain scission rate is no longer time dependent, and eq 21 can be solved analytically. The fraction of nonbroken chains decays exponentially,

$$n(t) = e^{-N_b\nu(\epsilon)t} \qquad (24)$$

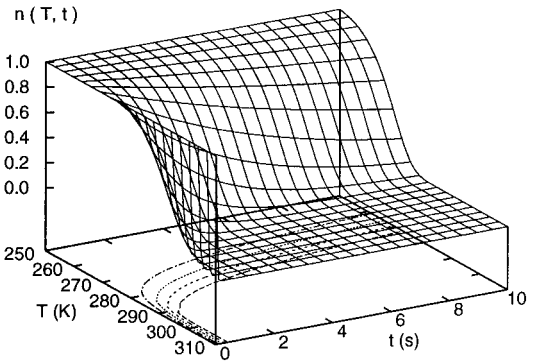

Figure 9. Fraction of nonbroken chains for a fiber at constant strain is plotted as a function of time and temperature. The chains contain 10 000 CC bonds and are subjected to a strain of 0.079. The contours $n = 0.2$, 0.4, 0.6, and 0.8 are shown in the ground plane of the figure.

The definition of the time of fracture can be chosen the same as in the constant strain rate case but has less physical meaning. The scission rate is temperature-dependent (eq 1) and leads to a temperature-dependent decay. Figure 9 shows the number of nonbroken chains as a function of time for different temperatures. The fiber is subjected to a strain of 0.079, and each chain contains $N_b = 10\,000$ bonds. The influence of temperature is significant, but there is no sharp change in the time of fracture. This means that in the case of this model for scission there is no first-order phase transition.

6. Discussion and Conclusion

In this paper we have focused on the bond scission mechanism, one of the possible microscopic mechanisms behind failure of polyethylene fibers. The energy barrier was calculated with an effective potential method and depends quadratically on the stress. A purely ab initio search for the transition state gave the same barrier heights, confirming the validity of the former approach. The results are in qualitative agreement with the results of Crist et al.,[15] which is expected since our model is an extended version of theirs.

The dependence on the stress/strain is considerable. The barrier is halved at a strain of 4.4% and is reduced to a third for a strain of 7%. The main reason for this strong reduction is the term $f\Delta L$. This term is, in the case of a constant external force, equivalent to the work done during the scission process, i.e., going from the initial state to the transition state. In the case of a constant strain on an infinite chain, this term mimics the relaxation of the chain as a whole during the process. It is clear that this term cannot be neglected and plays an important role.

The calculated bond scission rate can be used to make a comparison with the experiment of Wang et al.[16] From the amount of radicals detected during their experiment an average scission rate can be estimated by dividing by the total time and the total number of bonds. This leads to a scission rate of 5.4×10^{-14} s^{-1}, which corresponds with an energy barrier of 1.70 eV if the prefactor $\Omega = 2.1 \times 10^{15}$ s^{-1} is used. That this is clearly much lower than the strength of a CC bond, which is 4 eV, can (to a large extent) be explained by the strong strain dependence of the barrier. A strain of 5.3% is sufficient to lower the energy barrier to 1.70 eV. This strain is larger than the observed microscopic strains in polyethylene (2.5%).[36] This discrepancy is not unreasonable, since we did not incorporate defects like CH_3 side groups, nor stress concentration effects. Their inclusion will lower the barrier from theory. Hence, the microscopic strain that has to be applied to the theoretical fiber without defects will be too large. This result supports the approach presented for the description of chain scission.

The scission rate is also used to calculate the behavior of a polyethylene fiber consisting of independent chains in a constant strain rate experiment. The strains at failure are 7−8%, which can be seen as an estimate of the ultimate strain. They are a factor of 3 larger than the observed microscopic strains in experiment. This is an important improvement compared to previous ab initio values,[6,7] which differed more than a factor of 8. Inclusion of defects and interchain interactions in the calculation could answer the question whether defects are responsible for the remaining discrepancy or whether a more accurate quantum mechanical approach is necessary.

It has to be stressed that the activation energy (defined via the time to break) as found in our calculation is as low as in the constant strain rate experiments. Although it is often believed that low activation energies are an indication for chain slip, our model demonstrates that chain scission can give similar results.

Our point of view may seem in disagreement with that of Smith,[13,14] who has proposed, on purely thermodynamical grounds, that polyethylene fibers will fracture by a local melting procedure (chain slip). From that theory, he has made reasonable estimates for the maximal strains that can be applied on polyethylene fibers. However, thermodynamics alone cannot provide a microscopic mechanism or an explanation for the radical formation observed in experiment.

On the other hand, in this paper we have shown that a microscopic theory based on scission leads to failure at strains which are a factor of 2−3 larger than in experiments. Activation energies are found in the order of the experimental values. The scission process could explain the amount of radicals. However, the concept of defects will have to be introduced to lower the microscopic strain at failure to the experimental observed strains.

From the temperature dependence of the time to break it follows that the scission process, as described by the microscopic theory, does not lead to a first-order phase transition. For this reason it is concluded that the thermodynamic theory and the microscopic theory are not equivalent.

In conclusion, on the basis of the results presented, it is likely that chain scission plays an important role in the failure of highly oriented polyethylene fibers.

Acknowledgment. We thank Prof. B. Crist Jr. for his useful comments. This work is part of the research program of the Stichting voor Fundamenteel Onderzoek der Materie (FOM) with financial support from the Nederlandse Organisatie voor Wetenschappelijk Onderzoek (NWO).

References and Notes

(1) Prevorsek, D. *Encycl. Polym. Sci. Eng. [Suppl. Vol.]* **1991**, 803.
(2) Meier, R. J. *Macromolecules* **1993**, *26*, 4376.
(3) Crist, B.; Hereña, P. G. *J. Polym. Sci., Part B: Polym. Phys.* **1996**, *34*, 449.

(4) Hageman, J. C. L.; Meier, R. J.; Heinemann, M.; de Groot, R. A. *Macromolecules* **1997**, *30*, 5953.
(5) Barham, P. J.; Keller, A. *J. Polym. Sci., Polym. Lett. Ed.* **1979**, *17*, 591.
(6) Suhai, S. *J. Chem. Phys.* **1986**, *84*, 5071.
(7) Crist, B.; Ratner, M. A.; Brower, A. L.; Sabin, J. R. *J. Appl. Phys.* **1979**, *50*, 6047.
(8) Boudreaux, D. S. *J. Polym. Sci., Polym. Phys. Ed.* **1973**, *11*, 1285 has reported values of 19 GPa at 33% strain, but at a very low level of accuracy.
(9) Savatskii, A. V.; Gorshkova, I. A.; Demicheva, V. P.; Frolova, I. L.; Shmikk, G. N. *Polym. Sci. USSR* **1984**, *26*, 2007.
(10) Porter, R. S.; Kanamoto, T.; Zachariades, A. E. *Polymer* **1994**, *35*, 4979.
(11) Wang, J.; Smith, K. J. *Polymer* **1999**, *40*, 7261.
(12) Kausch, H. H.; Becht, J. The role of intra- and intermolecular cohesion in fracture initiation of high polymers. In *Deformation and Fracture of High Polymers*; Kaush, H. H., Hassell, J. A., Jaffee, R. I., Eds.; Plenum Press: New York, 1974.
(13) Smith, K. J. *Polym. Sci. Eng.* **1990**, *30*, 437.
(14) Smith, K. J.; Wang, J. *Polymer* **1999**, *40*, 7251.
(15) Crist, B.; Oddershede, J.; Sabin, J. R.; Perram, J. W.; Ratner, M. A. *J. Polym. Sci., Polym. Phys. Ed.* **1984**, *22*, 881.
(16) Wang, D.; Klaassen, A. A. K.; Janssen, G. E.; de Boer, E.; Meier, R. J. *Polymer* **1995**, *36*, 4193.
(17) Saitta, A. M.; Klein, M. L. *J. Chem. Phys.* **1999**, *111*, 9434.
(18) The atoms are treated as classical particles. The effect of treating the atomic coordinates, excluding the reaction coordinate, quantum mechanically is estimated in section 4.2 using the quantum mechanical partition function.
(19) Actually, the validity of this assumption follows from the assumption that the chain can be divided into segments. Then, the boundary of the segment defined by L, and the internal coordinates of the segment give the energy and stress. Requirement of zero forces (extremum of energy) and the fact that the extrema with lowest energy can be discriminated by l_c, apart from degeneracies, define the breaking segment.
(20) Kresse, G.; Hafner, J. *Phys. Rev. B* **1993**, *47*, 558; **1994**, *49*, 14251.
(21) Kresse, G.; Furthmüller, J. *Comput. Mater. Sci.* **1996**, *6*, 15.
(22) Kresse, G.; Furthmüller, J. *Phys. Rev. B* **1996**, *54*, 11169.
(23) Perdew, J. P.; Chevary, J. A.; Voska, S. H.; Jackson, K. A.; Pederson, M. R.; Singh, D. J.; Fiolhais, C. *Phys. Rev. B* **1992**, *46*, 6671.
(24) Vanderbilt, D. *Phys. Rev. B* **1990**, *41*, 7892. These pseudopotentials are softer than the ones used in previous work,[4] reducing the cutoff energy from 54 to 26 Ry.
(25) Kerr, J. A. *Chem. Rev.* **1966**, *66*, 465.
(26) Pople, J. A.; Schlegel, H. B.; Krishnan, R.; Defrees, D. J.; Binkley, J. S.; Frisch, M. J.; Whiteside, R. A.; Hout, R. F.; Hehre, W. J. *Int. J. Quantum Chem. Symp.* **1981**, *15*, 269.
(27) Jacox, M. E. *J. Phys. Chem. Ref. Data* **1990**, *19*, 387.
(28) Murnaghan, F. D. *Proc. Natl. Acad. Sci. U.S.A.* **1944**, *3*, 244.
(29) The value of 334 GPa mentioned in the Introduction was for an area at 4 K.
(30) Hageman, J. C. L.; van der Horst, J. W.; de Groot, R. A. *Polymer* **1999**, *40*, 1313.
(31) The reader, who would like to use the presented scheme, is cautioned that for very low strains the transition state is found in a larger unit cell: going to lower strains, the breaking bond will at a certain point increase more (it can go to infinity) than the all other bonds will shrink, since they have to have positive strain. This implies that there is a minimal length L^*, below which no transition state exists.
(32) Kresse, G.; Furthmüller, J.; Hafner, J. *Europhys. Lett.* **1995**, *32*, 729.
(33) An additional correction to the dynamical matrix has been applied since residual interchain interactions led to a spurious imaginary rotation mode in the spectra. The calculated force constants are adjusted in such a way that only the energy of this specific mode was shifted to zero at Γ.
(34) Wool, R. P.; Bretzlaff, R. S. *J. Polym. Sci., Part B: Polym. Phys.* **1986**, *24*, 1039.
(35) Prasad, K.; Grubb, D. T. *J. Polym. Phys., Part B* **1989**, *27*, 381.
(36) Moonen, J. A. H. M.; Roovers, W. A. C.; Meier, R. J.; Kip, B. J. *J. Polym. Sci., Polym. Phys. Ed.* **1992**, *30*, 361.
(37) Meier, R. J.; Vansweefelt, H. *Polymer* **1995**, *36*, 3825.
(38) Smith, P.; Lemstra, P. *J. Mater. Sci.* **1980**, *15*, 505.
(39) Zhurkov, S. N.; Kuksenko, V. S.; Slutsker, A. I. In *Proceedings of the Second International Conference on Fracture*, Brighton, 1969; p 531.

MA000682A